ADVANCED MATERIALS TECHNOLOGIES
www.advmattechnol.de

A Monodisperse, End-Capped Ru(bda) Oligomer with Outstanding Performance in Heterogeneous Electrochemical Water Oxidation

Tilman Schneider, Florian Seebauer, Florian Beuerle, and Frank Würthner**

Water oxidation catalysis is a key step for sustainable fuel production by water splitting into hydrogen and oxygen. The synthesis of a novel coordination oligomer based on four Ru(bda) (bda = 2,2′-bipyridine-6,6′-dicarboxylate) centers, three 4,4′-bipyridine (4,4′-bpy) linkers, and two 4-picoline (4-pic) end caps is reported. The monodispersity of this tetranuclear compound is characterized by NMR techniques. Heterogeneous electrochemical water oxidation after immobilization on multi-walled carbon nanotubes (MWCNTs) shows catalytic performance unprecedented for this compound class, with a turnover frequency (TOF) of 133 s^{-1} and a turnover number (TON) of 4.89×10^6, at a current density of 43.8 mA cm^{-2} and a potential of 1.45 V versus normal hydrogen electrode (NHE).

1. Introduction

The development of sustainable and carbon-neutral energy sources is essential for the transformation of the worldwide energy system in response to man-made climate change.[1] However, the usage of renewable energy harvested by solar cells or wind turbines is currently still hampered by limited storage capacities for electricity.[2] One promising alternative is chemical energy storage, e.g., the production of green hydrogen by electrochemical water splitting.[3] In order to facilitate this process, the search for efficient and stable catalysts is ongoing.[4] For direct water splitting, the O_2-evolving oxidative half-reaction is the most challenging part because the energetically uphill four-electron process requires rigorous operation conditions.[1,5] Organometallic ruthenium complexes offer a broad variety of mono- and multinuclear structures with intriguing spectroscopic and electronic properties,[6] giving rise to a plethora of potential applications in homogeneous and heterogeneous environments.[7] Consequently, molecular Ru-based water oxidation catalysts (WOCs) emerged as the most promising class of catalysts with outstanding activity and stability.[5] Pioneering work in this area was already done in the 1980s, e.g., with the introduction of the first RuWOC by Meyer and co-workers.[8] The whole field was however rejuvenated in the 2000s and has continuously advanced ever since, with mononuclear,[9] dinuclear,[10] macrocyclic,[11] and polymeric[12] complexes being applied in photo-[13] or electrochemical[14] variants.

In this regard, heterogeneous electrochemical water oxidation is particularly interesting due to straightforward setups, high stability of the catalysts, and the low amount of required active materials.[15] Typically, turnover numbers (TONs) for electrochemical water oxidation exceed values for chemical or photochemical catalysis by several orders of magnitude.[14a] In order to facilitate charge transport and injection into electrodes, immobilization of molecular WOCs on multi-walled carbon nanotubes (MWCNTs) is particularly promising due to the high conductivity of the nanotubes and the possibility for highly stable anchoring of the WOCs via CH–π and π–π interactions.[16] Thereby, high loading, and thus, current density, but also excellent catalyst stability was achieved with both molecular[14b,16a,17] and polyoxometalate[18] catalysts.

Recently, a trinuclear Ru(bda) macrocycle (bda = 2,2′-bipyridine-6,6′-dicarboxylate)[14b] and a linear Ru-based coordination polymer[17a] were introduced as promising examples of multinuclear Ru-based catalysts for heterogeneous electrochemical water oxidation. To gain deeper insight into structure–activity relationships for such electrochemical WOCs, we aimed for the synthesis of small monodisperse linear oligomers. Here, we report the synthesis and characterization of linear Ru(bda) oligomer **1** with composition $[(Ru(bda))_4(4,4'\text{-bpy})_3pic_2]$ (4,4′-bpy = 4,4′-bipyridine, pic = 4-picoline). Heterogeneous electrocatalysis after coating of glassy carbon (GC) electrodes with **1** on MWCNT support showed excellent turnover frequency (TOF) and TON for water oxidation.

T. Schneider, F. Seebauer, F. Beuerle, F. Würthner
Institut für Organische Chemie
Universität Würzburg
Am Hubland, 97074 Würzburg, Germany
E-mail: florian.beuerle@uni-tuebingen.de; wuerthner@uni-wuerzburg.de
F. Beuerle
Institut für Organische Chemie
Universität Tübingen
Auf der Morgenstelle, 72076 Tübingen, Germany

The ORCID identification number(s) for the author(s) of this article can be found under https://doi.org/10.1002/admt.202301721

DOI: 10.1002/admt.202301721

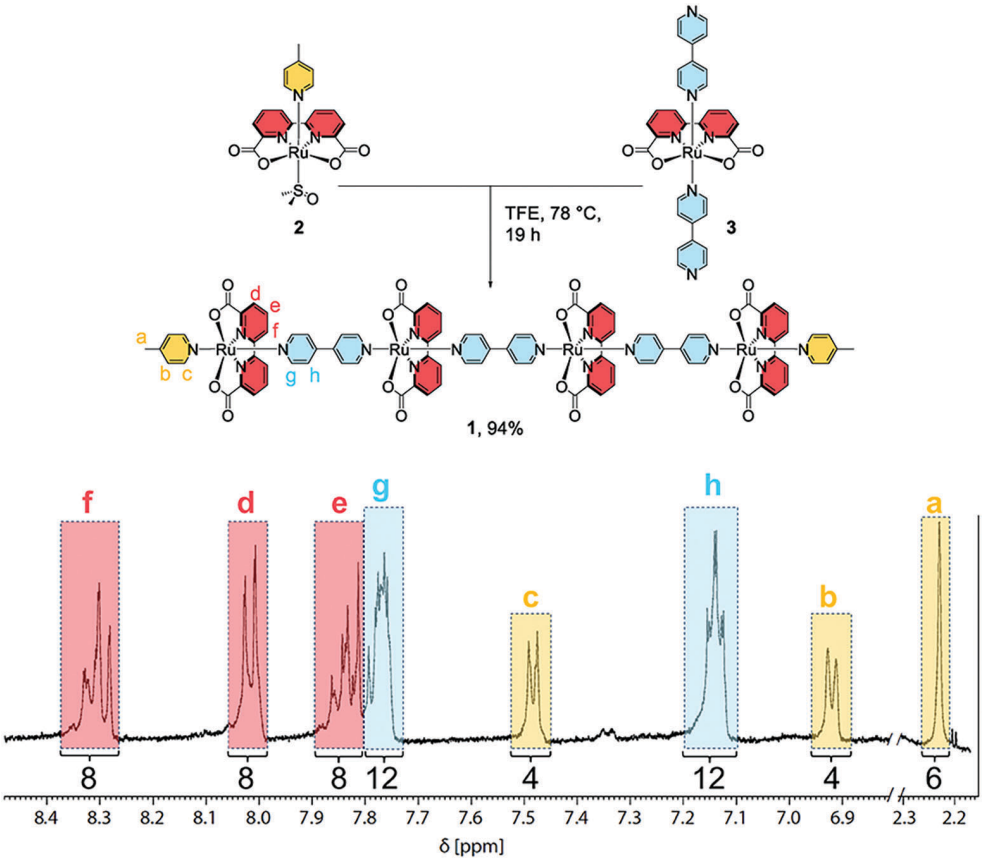

Figure 1. Synthesis of **1** starting from Ru(bda)(dmso)(pic) (**2**) and Ru(bda)(4,4′-bpy)$_2$ (**3**) and ^{1}H NMR spectrum (400 MHz, CD_2Cl_2/F_3CCD_2OD 9:1, ascorbic acid) of **1** with integration of protons for length determination by end-group analysis.

2. Results and Discussion

2.1. Synthesis and Characterization

Our previous research[14b,17a] suggested that sufficient extension of Ru(bda) oligomers is required for stable binding to the π surface by van der Waals interactions. Accordingly, we were not sure if a Ru(bda) trimer formed by a modular approach from the literature-known end cap unit Ru(bda)(dmso)(pic) (**2**)[19] and the central connection unit Ru(bda)(4,4′-bpy)$_2$ (**3**)[20] would form sufficiently stable linkage to MWCNTs. However, much to our surprise, the reaction of the two building blocks in 2:1 ratio in 2,2,2-trifluoroethanol (TFE) at 80 °C[21] for 19 h (**Figure 1**) afforded the tetranuclear Ru(bda) oligomer **1** in 94% yield (based on starting material **3**).

Thanks to the poor solubility of Ru oligomer **1**, facile purification of the crude product was achieved by evaporation of the reaction mixture and sequential washing with MeOH, CH_2Cl_2, Et_2O, and *n*-pentane. The chemical composition of the oligomer was confirmed by ^{1}H NMR end-group analysis (Figure 1). Integer ratios between protons from the pic, bda, and linker moieties indicate a pure tetranuclear complex with sum formula [Ru(bda)]$_4$(4,4′-bpy)$_3$pic$_2$. To determine the molecular size and to further validate the chemical composition, diffusion-ordered NMR spectroscopy (DOSY) was measured. The well-defined trace in the 2D plot (Figure S1, Supporting Information) and the excellent agreement of the experimental decay curves with a monoexponential fit (diffusion coefficient $D = 3.84 \times 10^{-10}$ m^2 s^{-1}) suggest that the sample consists of only one molecular species. By contrast, the application of the log-normal fitting model[22] for polydisperse samples was not feasible (see example in Figure S3, Supporting Information). Due to the prolate shape of this structure, the spherical particle approach of the Stokes–Einstein equation is not applicable,[23] which is why we used a cylindrical model introduced by Tirado et al.[24] to estimate the aspect ratio and molecular dimensions of **1**. Based on molecular modeling (Figures S5 and S6, Supporting Information) and literature data,[17a] the width of the oligomer chain was estimated based on the width of one bda unit and fixed at 0.91 nm. A length of 5.60 nm was thus calculated for oligomer **1** (Figure S4, Supporting Information), which is in good agreement with a molecular structure obtained from force field calculations (UFF, Materials Studio).[25] Based on this combined analytical data, axial ligand scrambling appears to occur under our reaction conditions, leading to monodisperse tetranuclear Ru complex **1** as the only isolable product.

Whereas solid samples of **1** can be stored for prolonged times, ^{1}H NMR spectroscopy in organic solvents indicated decomposition of the Ru complexes within a few hours. Limited stability of the coordinative Ru—N bonds in solution was also observed in ESI mass spectrometry, as only fragments with up to two Ru(bda) units were detected (Figure S11, Supporting Information).

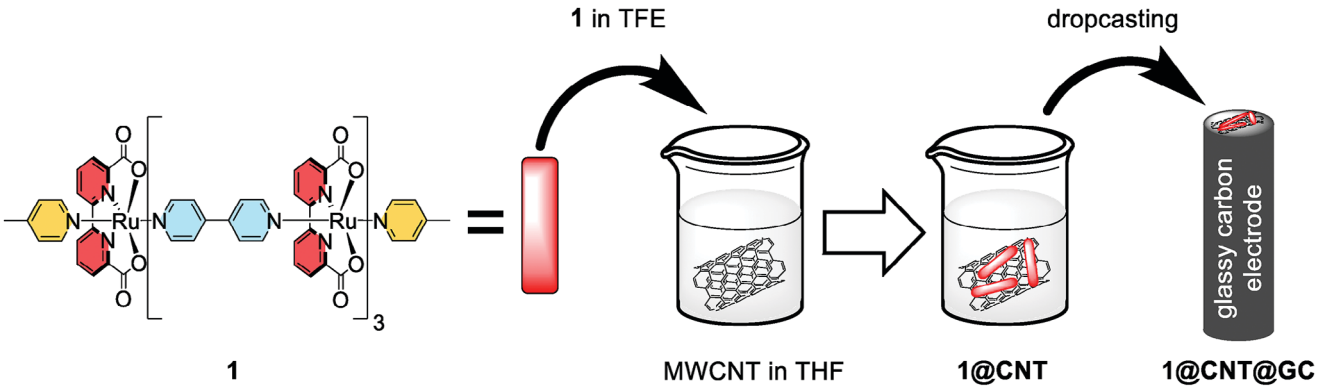

Figure 2. Preparation process of the glassy carbon electrodes.

2.2. Electrochemical Water Oxidation

Due to a—compared to our trinuclear macrocycles[14b]—extended size of the tetranuclear oligomer **1** and its poor solubility, we envisioned good adhesion and high performance as active electrode material in electrochemical water oxidation. For better conductivity and charge injection,[16a] **1** was initially immobilized on MWCNTs by adding a TFE solution (100 µL, 1 mg mL^{-1}) of the oligomeric WOC to a THF dispersion of MWCNTs (1 mL, 1 mg mL^{-1}) prepared by ultrasonication (**Figure 2**). Instant decolorization of the supernatant solution indicated successful anchoring of the WOC on the MWCNTs to form hybrid material **1@CNT**, which was further analyzed by scanning electron microscopy (SEM) and energy-dispersive X-ray spectroscopy (EDX) (Figure S9, Supporting Information). In contrast, immobilization of the monomeric precursors **2** or **3** on MWCNTs was not possible, as the solution was still intensely colored after any deposition attempts. This observation clearly highlights the importance of a multinuclear structure for stable anchoring. Electrodes **1@CNT@GC** were prepared by dropcasting a **1@CNT** dispersion (4 × 20 µL in THF/TFE) on GC electrodes until the electrode surface was covered by a continuous layer of **1@CNT** (see Figure 2 and Supporting Information for details).

Subsequently, the electrochemical performance of **1@CNT@GC** electrodes was analyzed by various analytical techniques. The setup consisted of a glass vial filled with phosphate buffer (phbf) solution (1 M ionic strength) as electrolyte, **1@CNT@GC** working electrode, $Hg/HgSO_4$ reference electrode, and platinum mesh counter electrode. Noncatalytic waves for the $Ru^{III/II}$, $Ru^{IV/III}$, and $Ru^{V/IV}$ oxidations were observed at around 700, 820, and 1070 mV versus normal hydrogen electrode (NHE), respectively (**Figure 3a**). The current density of the catalytic wave was initially quite low but increased significantly after activation by 100 consecutive cyclic voltammetry (CV) cycles (Figure 3b,c). During activation, the $Ru^{III/II}$ wave remains around 710 mV but drops significantly in intensity, while the $Ru^{IV/III}$ wave shifts to around 900–950 mV, and the $Ru^{V/IV}$ wave disappears below the intensifying catalytic wave. Based on previous observations,[17a] we assume that the catalytically active species[14b,17] is only formed after partial dissociation of the bda ligand upon electrochemical activation. This allows the alignment of one carboxypyridine unit with the MWCNT surface, thereby enhancing the surface binding by replacing weaker CH–π with stronger π–π interactions. Meanwhile, this rearrangement of the equatorial ligand upon electrochemical activation stabilizes higher oxidation states at the Ru centers, facilitating the binding of additional water molecules and, thus, enhancing the catalytic performance.[17a] While the activated state of **1@CNT@GC** is stable for some time, controlled potential electrolysis (CPE) measurements of activated electrodes that were stored at ambient conditions for several hours before the measurement, again displayed a slight increase in current density for the initial cycles, which indicates that the activated WOCs slowly convert back to the original state, but can be reactivated.

In **Table 1**, the averaged electrocatalytic properties of **1** are summarized and compared with benchmark examples from the literature. Intriguingly, oligomeric WOC **1** showed unprecedented activity and stability even at low catalyst loading.

The obtained overpotential of 358 mV approaches the theoretical minimum of around 300 mV for catalysts following the water nucleophilic attack (WNA) mechanism[26] and compares well with reported values for similar catalysts (entries 2, 4, and 7 in Table 1).

Surface coverage of **1@CNT@GC** was determined by the integration of a noncatalytic CV wave. On average, 0.8 nmol cm^{-2} of active Ru sites were found, which is lower than for longer oligomers or rigid macrocycles (entries 2, 3, 7 in Table 1) but comparable to electrodes modified with molecular WOCs (entries 4, 5, 6 in Table 1).

To estimate the catalytic activity, several methods have been proposed for the calculation of catalytic rates[16a,27] and one must carefully distinguish the information that is conveyed. By foot of the wave analysis (FOWA) calculations, the apparent rate constant k_{WNA} can be determined for systems following a hetero-WNA mechanism, as it is assumed for WOC **1**.[9c,27a] In the limit of infinite potential, k_{WNA} equals the maximum possible turnover frequency TOF_{max} for the water oxidation process.[17a,27b] On the other hand, the actual TOF at defined experimental conditions can be determined using the modified expression of Faraday's law in Equation 1

$$TOF = \frac{J}{n \cdot F \cdot \Gamma_{cat}} \quad (1)$$

Table 1. Comparison of electrochemical data for **1** (average values obtained from several measurements) with state-of-the-art materials from literature.

Entry	WOC	Γ[a] [nmol cm^{-2}]	E[b] [V]	J[c] [mA cm^{-2}]	E_{onset}[d] [mV]	k_{WNA}[e] [s^{-1}]	TOF [s^{-1}]	TON[f]
1	**1@CNT@GC**	0.80	1.45	43.8	358	6.46×10^3	133	4.89×10^6
2	**MC3@CNT@GC**[14b]	8.40	1.45	186	330	3.30×10^3	23.0[g]	6.00×10^5
3	**[Ru(bda)(H$_2$O)$_2$]$_{10}$(4,4′-bpy)$_{11}$@CNT@GC**[17a]	16.7	1.45	256	-	3.70×10^3	2.30[g]	9.40×10^3
4	**Ru(bda)(pyn)$_2$@CNT@ITO**[16a]	2.00	1.80	0.72	280	-	0.30	1.10×10^4
5	**Ru(tda)(Pyr-Py)$_2$@CNT@GC**[27b]	0.03	1.45	2.20	-	8.07×10^3	40.0	1.20×10^6
6	**Ru(tda)(pyn)$_2$@CNT@GC**[27b]	0.55	1.45	10.5	-	8.90×10^3	49.5[g]	6.70×10^5
7	**[Ru(OH$_2$)(tda)]$_{15}$(4,4′-bpy)$_{16}$@CNT@GC**[17b]	17.5	1.45	240	440	8.06×10^3	0.44[g]	7.80×10^4

[a] active metal sites loading [b] operation voltage versus NHE [c] maximum current density [d] onset overpotential [e] equals TOF$_{max}$, determined by the foot of the wave analysis (FOWA) [f] TON per Ru center [g] calculated in the course of this work from available literature data as value was not reported in in original publication.

with J = current density, n = number of electrons (4 in case of water oxidation) F = Faraday constant, and Γ_{cat} = surface coverage of active metal sites per cm^2.[27c]

For a better comparison with benchmark examples from the literature, both methods have been applied to **1@CNT@GC**. While FOWA (**Figure 4a**) gave apparent rate constants k_{WNA} in the range of 6.46×10^3 s^{-1} per Ru center, a TOF of 133 s^{-1} per Ru center was obtained as an average from several measurements. For both parameters, the activity of **1** is much higher compared to mononuclear bda complexes or macrocycle **MC3** (entries 2–4 in Table 1), possibly due to higher accessibility of the water binding sites in comparison with the somewhat more restricted macrocyclic structure of **MC3**. Regarding k_{WNA}, oligomer **1** is even in the range and only slightly less active than WOCs with the intrinsically more active equatorial tda ligand (entries 5–7 in Table 1).[14a] Intriguingly, the unprecedented TOF value of **1@CNT@GC** is notably higher than any values from the literature and approaches the range of the oxygen-evolving complex in photosystem II (TOF = 100–400 s^{-1}).[9c]

Faraday efficiency was determined by quantitative O_2 detection during CPE experiments, for which an airtight two-compartment cell was used to separate the working and counter electrodes. To produce sufficient amounts of O_2, a catalyst-coated GC plate (1 cm^2) was used as the working electrode. The evolved gaseous O_2 in the cell headspace was detected by a Clark electrode sensor and an excellent Faraday efficiency of 95% was calculated in relation to the theoretical maximum yield predicted from CPE measurements (Figure 4b). The following TON determination was carried out assuming a charge-to-O_2 conversion efficiency of 100%, which was justified by the previous findings. CPE experiments revealed a current density of around 35 mA cm^{-2}, which remained constant for over 12 h (Figure 4c), while even higher peak current densities (on average 44 mA cm^{-2}) were observed for short durations in CV. Therefore, a remarkably high TON of 4.89×10^6 per Ru(bda) unit was counted before the cutoff criterion of 90% current density related to the starting value was reached. To the best of our knowledge, this TON value surpasses any molecular Ru-based electrocatalyst known from literature so far. The typical mononuclear RuWOCs and most multinuclear structures are outperformed by two to three orders of magnitude,[16a,28] with only Ru(tda)(Pyr-Py)$_2$ (entry 4 in Table 1)[27b] being in the same range as **1**, presumably due to strong π–π interactions between its pyrene moieties and MWCNTs. We attribute this superior performance to a stabilizing effect of the picoline end caps. While literature-known oligomers/polymers possess potentially reactive free Ru(bda) binding sites at the ends,[17a] **1** is terminated by strongly coordinated monodentate picoline ligands. Thereby, one potential catalyst deactivation pathway via oligomer decomposition is suppressed. Intriguingly, the TON is also about one order of magnitude higher than for previously reported electrodes with macrocyclic **MC3** as catalyst.[14b] Based on the molecular structures, we propose that the conformational rigidity of **MC3** limits the stability under operating conditions. Presumably, the restricted geometry of macrocyclic **MC3** hampers any conformational changes, which, however, are necessary to reach the activated state of the catalyst. In contrast, steric hindrance is less critical in the rather flexible oligomer **1**, which therefore exhibits both stronger binding to the MWCNTs and better accessibility of the reactive Ru sites. This assumption is in accordance with the experimental findings, as **1** surpasses **MC3** in both k_{WNA} and TON.

3. Conclusion

We have presented a straightforward synthetic protocol for a new monodisperse tetranuclear coordination oligomer **1** with composition [(Ru(bda))$_4$(4,4′-bpy)$_3$pic$_2$] by reaction between state-of-the-art Ru(bda) precursors **2** and **3** in TFE. Excellent performance in heterogeneous electrochemical water oxidation catalysis at neutral pH was observed even at low catalyst loading, with a very high k_{WNA} of around 6500 s^{-1}, as well as new record TOF of 133 s^{-1} and TON of more than 4.8 million turnovers per active metal site. This outstanding performance is achieved by a combination of several beneficial properties. Strong adhesion to the electrode surface is maintained by the oligomeric structure with multiple anchoring sites and the poor solubility prohibits creeping detachment. The durability of the system is enhanced by the inert 4-picoline end caps, which serve as protective groups to diminish deactivation pathways via gradual axial ligand dissociation.

The combination of high catalytic performance and unprecedented stability for oligomeric WOC **1** as electrode support in electrochemical water oxidation paves the way for device integration and further investigations under true operating conditions. These exciting initial findings will help to identify and further optimize well-defined molecular WOCs that may compete with and outperform metal oxides in large-scale applications.

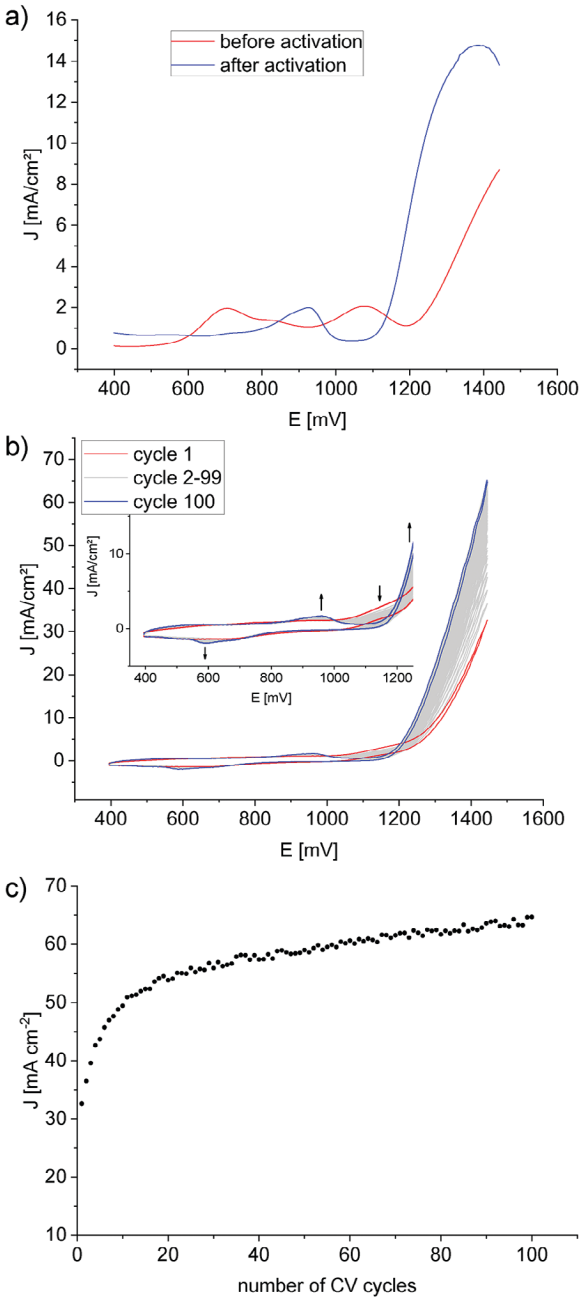

Figure 3. Activation of **1@CNT@GC** (1 M phbf, pH 7; scan rate: 100 mV s^{-1}; range: 0.395–1.445 V versus NHE): a) differential pulse voltammetry (DPV) (red: before activation; blue: after activation); b) CV (red: cycle 1; grey: cycles 2–99; blue: cycle 100; inset: magnification of noncatalytic waves); c) peak current density plotted against the number of activation cycles.

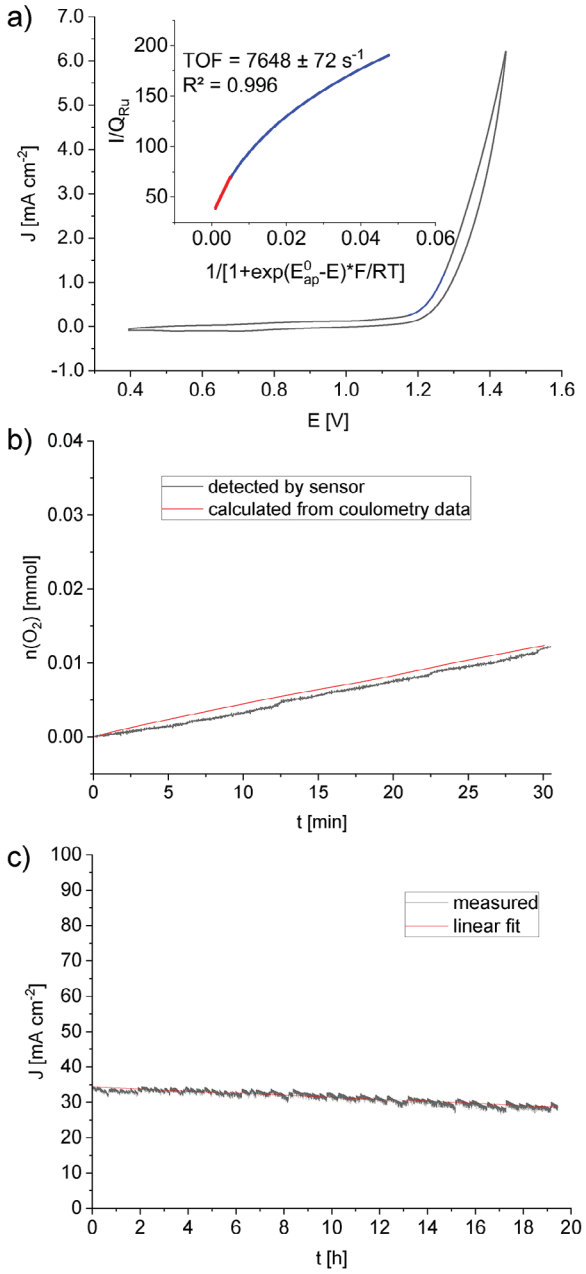

Figure 4. Electrochemical analysis of **1@CNT@GC**: a) determination of k_{WNA} by FOWA from CV data (1 M phbf, pH 7; scan rate: 100 mV s^{-1}; range: 0.395–1.445 V); blue line marks the input data for FOWA (inset: plot after FOWA calculations with linear fit to obtain k_{WNA}); b) CPE experiment for determination of the Faraday efficiency (1 M phbf, pH 7; 1.405 V); black: O_2 detected by sensor. red: theoretical maximum calculated from expended charge; c) CPE experiment (1 M phbf, pH 7; 1.445 V) for stability determination.

4. Experimental Section

Materials: All reactions were carried out in standard glass equipment. All chemicals were purchased from usual commercial suppliers and used without further purification, unless stated otherwise. Conventional solvents were distilled prior to use.

*Synthesis of [(Ru(bda))$_4$(4,4′-dipyridyl)$_3$(4-picoline)$_2$] **1***: A Schlenk tube was charged with **2**[19] (33.2 mg, 64.5 µmol, 2.1 eq.) and **3**[20] (20.0 mg, 30.7 µmol, 1.0 eq.) and dissolved in degassed TFE (4.0 mL). The mixture was heated to reflux for 19 h under an inert atmosphere of argon. The solvent was removed under reduced pressure and the residue was washed several times with methanol, DCM, Et_2O, and *n*-pentane (50 mL each). **Yield**: 38.8 mg (19.1 µmol, 94%) of a dark red solid. **Chemical Formula**: $C_{90}H_{62}N_{16}O_{16}Ru_4$. **M.p.**: > 400 °C. **^{1}H-NMR** (600 MHz, CD_2Cl_2:CF_3CD_2OD 9:1, ascorbic acid): δ = 8.33–8.28 (m, 8H, H_f), 8.03–

7.99 (m, 8H, H_d), 7.85–7.80 (m, 8H, H_e), 7.78–7.74 (m, 12H, H_g), 7.49 (d, $^3J = 6.2$ Hz, 4H, H_c), 7.17–7.14 (m, 12H, H_h), 6.92 (d, $^3J = 6.2$ Hz, 4H, H_b), 2.23 (s, 6H, H_a) ppm. Anal. calc. for $C_{90}H_{62}N_{16}O_{16}Ru_4$ (2027.86): C 53.31, H 3.08, N 11.05; found: C 52.17, H 2.97, N 11.04.

Supporting Information

Supporting Information is available from the Wiley Online Library or from the author.

Acknowledgements

This project has received funding from the European Research Council (ERC) under the European Union's Horizon 2020 research and innovation program (grant agreement no. 787937; recipient F.W.). The authors gratefully acknowledge financial support by the State of Bavaria within the initiative "Solar Technologies go Hybrid (SolTech)". The authors thank Prof. Antoni Llobet and Dr. Dorothee Schindler for helpful discussions concerning all aspects of electrocatalysis. T. S. would like to thank Svetlana Ivanova, Stefanie Schmitt, and Theresa Zorn for helpful discussions and assistance concerning diffusion NMR measurements, Dr. Vladimir Stepanenko for recording electron microscopy data, and Dr. Tim Schlossarek for assistance with molecular modeling.

Open access funding enabled and organized by Projekt DEAL.

Conflict of Interest

The authors declare no conflict of interest.

Data Availability Statement

The data that support the findings of this study are openly available in [Zenodo] at [https://doi.org/10.5281/zenodo.8415310], reference number [8415310].

Keywords

coordination oligomers, electrocatalysis, heterogeneous catalysis, renewable fuels, ruthenium bda complexes, water oxidation catalysis, water splitting

Received: October 9, 2023
Revised: December 16, 2023
Published online: January 4, 2024

[1] B. Zhang, L. Sun, *Chem. Soc. Rev.* **2019**, *48*, 2216.
[2] a) H. Chen, T. N. Cong, W. Yang, C. Tan, Y. Li, Y. Ding, *Prog. Nat. Sci.* **2009**, *19*, 291; b) T. M. Gür, *Energy Environ. Sci.* **2018**, *11*, 2696.
[3] a) D. J. Jovan, G. Dolanc, *Energies* **2020**, *13*, 6599; b) M. Thangamuthu, Q. Ruan, P. O. Ohemeng, B. Luo, D. Jing, R. Godin, J. Tang, *Chem. Rev.* **2022**, *122*, 11778.
[4] a) F. Puntoriero, G. La Ganga, A. M. Cancelliere, S. Campagna, *Curr. Opin. Green Sustain. Chem.* **2022**, *36*, 100636; b) F. Lucarini, J. Fize, A. Morozan, F. Droghetti, E. Solari, R. Scopelliti, M. Marazzi, M. Natali, M. Pastore, V. Artero, A. Ruggi, *Sustain. Energy Fuels* **2023**, *7*, 3384; c) E. Benazzi, V. Cristino, R. Boaretto, S. Caramori, M. Natali, *Dalton Trans.* **2021**, *50*, 696.
[5] a) R. Matheu, P. Garrido-Barros, M. Gil-Sepulcre, M. Z. Ertem, X. Sala, C. Gimbert-Suriñach, A. Llobet, *Nat. Rev. Chem.* **2019**, *3*, 331; b) R. Matheu, M. Z. Ertem, C. Gimbert-Suriñach, X. Sala, A. Llobet, *Chem. Rev.* **2019**, *119*, 3453; c) B. Zhang, L. Sun, *J. Am. Chem. Soc.* **2019**, *141*, 5565.
[6] a) J. Maurer, B. Sarkar, W. Kaim, R. F. Winter, S. Zális, *Chem. Eur. J.* **2007**, *13*, 10257; b) A. Notaro, M. Jakubaszek, N. Rotthowe, F. Maschietto, R. Vinck, P. S. Felder, B. Goud, M. Tharaud, I. Ciofini, F. Bedioui, R. F. Winter, G. Gasser, *J. Am. Chem. Soc.* **2020**, *142*, 6066; c) D. Fink, N. Orth, M. Linseis, I. Ivanovic-Burmazovic, R. F. Winter, *Chem. Commun.* **2020**, *56*, 1062; d) G. E. Pieslinger, I. Ramírez-Wierzbicki, A. Cadranel, *Angew. Chem., Int. Ed.* **2022**, *61*, e202211747; e) A. Cadranel, J. H. Hodak, *J. Coord. Chem.* **2015**, *68*, 1452; f) A. Cadranel, P. Alborés, S. Yamazaki, V. D. Kleiman, L. M. Baraldo, *Dalton Trans.* **2012**, *41*, 5343.
[7] a) A. J. Morris, G. J. Meyer, E. Fujita, *Acc. Chem. Res.* **2009**, *42*, 1983; b) G. J. Meyer, *Inorg. Chem.* **2005**, *44*, 6852; c) K. Cui, A. V. Soudackov, M. C. Kessinger, J. Xu, G. J. Meyer, S. Hammes-Schiffer, *J. Am. Chem. Soc.* **2023**, *145*, 19321; d) D. Wang, R. N. Sampaio, L. Troian-Gautier, S. L. Marquard, B. H. Farnum, B. D. Sherman, M. V. Sheridan, C. J. Dares, G. J. Meyer, T. J. Meyer, *J. Am. Chem. Soc.* **2019**, *141*, 7926; e) G. La Ganga, F. Puntoriero, E. Fazio, M. Natali, F. Nastasi, A. Santoro, M. Galletta, S. Campagna, *Chem. Eur. J.* **2021**, *27*, 16904; f) M. Natali, A. Sartorel, A. Ruggi, *Front. Chem.* **2022**, *10*, 907510.
[8] S. W. Gersten, G. J. Samuels, T. J. Meyer, *J. Am. Chem. Soc.* **1982**, *104*, 4029.
[9] a) J. J. Concepcion, J. W. Jurss, J. L. Templeton, T. J. Meyer, *J. Am. Chem. Soc.* **2008**, *130*, 16462; b) L. Duan, A. Fischer, Y. Xu, L. Sun, *J. Am. Chem. Soc.* **2009**, *131*, 10397; c) L. Duan, F. Bozoglian, S. Mandal, B. Stewart, T. Privalov, A. Llobet, L. Sun, *Nat. Chem.* **2012**, *4*, 418; d) L. Duan, C. M. Araujo, M. S. G. Ahlquist, L. Sun, *Proc. Natl. Acad. Sci. U.S.A.* **2012**, *109*, 15584; e) Y. Xie, D. W. Shaffer, J. J. Concepcion, *Inorg. Chem.* **2018**, *57*, 10533; f) C. J. Richmond, R. Matheu, A. Poater, L. Falivene, J. Benet-Buchholz, X. Sala, L. Cavallo, A. Llobet, *Chem. Eur. J.* **2014**, *20*, 17282; g) L. Wang, L. Duan, Y. Wang, M. S. G. Ahlquist, L. Sun, *Chem. Commun.* **2014**, *50*, 12947.
[10] a) C. Sens, I. Romero, M. Rodríguez, A. Llobet, T. Parella, J. Benet-Buchholz, *J. Am. Chem. Soc.* **2004**, *126*, 7798; b) R. Zong, R. P. Thummel, *J. Am. Chem. Soc.* **2005**, *127*, 12802.
[11] a) M. Schulze, V. Kunz, P. D. Frischmann, F. Würthner, *Nat. Chem.* **2016**, *8*, 576; b) V. Kunz, J. O. Lindner, M. Schulze, M. I. S. Röhr, D. Schmidt, R. Mitric, F. Würthner, *Energy Environ. Sci.* **2017**, *10*, 2137; c) V. Kunz, M. Schulze, D. Schmidt, F. Würthner, *ACS Energy Lett.* **2017**, *2*, 288; d) A.-L. Meza-Chincha, J. O. Lindner, D. Schindler, D. Schmidt, A.-M. Krause, M. I. S. Röhr, R. Mitrić, F. Würthner, *Chem. Sci.* **2020**, *11*, 7654; e) D. Schindler, A.-L. Meza-Chincha, M. Roth, F. Würthner, *Chem. Eur. J.* **2021**, *27*, 16938.
[12] T. Schlossarek, V. Stepanenko, F. Beuerle, F. Würthner, *Angew. Chem., Int. Ed.* **2022**, *61*, e202211445.
[13] a) N. Noll, A.-M. Krause, F. Beuerle, F. Würthner, *Nat. Catal.* **2022**, *5*, 867; b) A. Vidal, F. Adamo, E. Iengo, E. Alessio, *Inorg. Chim. Acta* **2021**, *516*, 120143.
[14] a) R. Matheu, M. Z. Ertem, J. Benet-Buchholz, E. Coronado, V. S. Batista, X. Sala, A. Llobet, *J. Am. Chem. Soc.* **2015**, *137*, 10786; b) D. Schindler, M. Gil-Sepulcre, J. O. Lindner, V. Stepanenko, D. Moonshiram, A. Llobet, F. Würthner, *Adv. Energy Mater.* **2020**, *10*, 2002329.
[15] S. Lin, Y. Pineda-Galvan, W. A. Maza, C. C. Epley, J. Zhu, M. C. Kessinger, Y. Pushkar, A. J. Morris, *ChemSusChem* **2017**, *10*, 514.
[16] a) F. Li, B. Zhang, X. Li, Y. Jiang, L. Chen, Y. Li, L. Sun, *Angew. Chem., Int. Ed.* **2011**, *50*, 12276; b) W. Zhang, E. J. Meeus, L. Wang, L.-H. Zhang, S. Yang, B. De Bruin, J. N. H. Reek, F. Yu, *ChemSusChem* **2022**, *15*, 202102379; c) P. D. Tran, A. Le Goff, J. Heidkamp, B. Jousselme, N. Guillet, S. Palacin, H. Dau, M. Fontecave, V. Artero, *Angew. Chem., Int. Ed.* **2011**, *50*, 1371.
[17] a) M. Gil-Sepulcre, J. O. Lindner, D. Schindler, L. Velasco, D. Moonshiram, O. Rüdiger, S. Debeer, V. Stepanenko, E. Solano, F. Würthner, A. Llobet, *J. Am. Chem. Soc.* **2021**, *143*, 11651; b) M. A. Hoque, M. Gil-Sepulcre, A. De Aguirre, J. A. A. W. Elemans,

D. Moonshiram, R. Matheu, Y. Shi, J. Benet-Buchholz, X. Sala, M. Malfois, E. Solano, J. Lim, A. Garzón-Manjón, C. Scheu, M. Lanza, F. Maseras, C. Gimbert-Suriñach, A. Llobet, *Nat. Chem.* **2020**, *12*, 1060.

[18] A. Sartorel, M. Carraro, F. M. Toma, M. Prato, M. Bonchio, *Energy Environ. Sci.* **2012**, *5*, 5592.

[19] a) A. Ghaderian, J. Holub, J. Benet-Buchholz, A. Llobet, C. Gimbert-Suriñach, *Inorg. Chem.* **2020**, *59*, 4443; b) B. D. Sherman, Y. Xie, M. V. Sheridan, D. Wang, D. W. Shaffer, T. J. Meyer, J. J. Concepcion, *ACS Energy Lett.* **2017**, *2*, 124.

[20] Y. Jiang, F. Li, F. Huang, B. Zhang, L. Sun, *Chin. J. Catal.* **2013**, *34*, 1489.

[21] a) J.-P. Bégué, D. Bonnet-Delpon, B. Crousse, *Synlett* **2004**, *2004*, 18; b) M. Buck, *Q. Rev. Biophys.* **1998**, *31*, 297; c) R. Rajan, P. Balaram, *Int. J. Pept. Protein Res.* **1996**, *48*, 328.

[22] N. H. Williamson, M. Nydén, M. Röding, *J. Magn. Reson.* **2016**, *267*, 54.

[23] a) Y. Cohen, L. Avram, L. Frish, *Angew. Chem., Int. Ed.* **2005**, *44*, 520; b) R. Evans, G. Dal Poggetto, M. Nilsson, G. A. Morris, *Anal. Chem.* **2018**, *90*, 3987; c) A. Macchioni, G. Ciancaleoni, C. Zuccaccia, D. Zuccaccia, *Chem. Soc. Rev.* **2008**, *37*, 479.

[24] M. M. Tirado, C. L. Martínez, J. G. De La Torre, *J. Chem. Phys.* **1984**, *81*, 2047.

[25] BIOVIA, *BIOVIA Materials Studio*, Dassault Systèmes, San Diego, CA, USA, **2017**.

[26] J. Hessels, R. J. Detz, M. T. M. Koper, J. N. H. Reek, *Chem. Eur. J.* **2017**, *23*, 16413.

[27] a) R. Matheu, S. Neudeck, F. Meyer, X. Sala, A. Llobet, *ChemSusChem* **2016**, *9*, 3361; b) J. Creus, R. Matheu, I. Peñafiel, D. Moonshiram, P. Blondeau, J. Benet-Buchholz, J. García-Antón, X. Sala, C. Godard, A. Llobet, *Angew. Chem., Int. Ed.* **2016**, *55*, 15382; c) C. Costentin, J.-M. Savéant, *ChemElectroChem* **2014**, *1*, 1226.

[28] B. Das, E. A. Toledo-Carrillo, G. Li, J. Ståhle, T. Thersleff, J. Chen, L. Li, F. Ye, A. Slabon, M. Göthelid, T.-C. Weng, J. A. Yuwono, P. V. Kumar, O. Verho, M. D. Kärkäs, J. Dutta, B. Åkermark, *J. Mater. Chem. A* **2023**, *11*, 13331.